3D split-step wavelet method for the propagation over impedance ground condition

Thomas Bonnafont, Rémi Douvenot, Alexandre Chabory

URSI GASS 2021, Rome, Italy, 28 August - 4 September 2021

3D split-step wavelet method for the propagation over impedance ground condition

T. Bonnafont*(1), R. Douvenot(2), and A. Chabory(2)
(1) Université de Pau & des Pays de l'Adour/E2s, Laboratoire SIAME, Pau, France (thomas.bonnafont@univ-pau.fr)
(2) ENAC, Université de Toulouse, France

Abstract

The long-range propagation of electromagnetic waves over the ground is a major topic for many applications in communication, navigation, and surveillance. In this article, we propose a wavelet-based split-step method in 3D to compute the propagation in this context. Also, using the discrete-mixed Fourier transform (DMFT), transverse invariant impedance ground conditions are taken into account, for which the ground wave propagation is accurately computed. Numerical tests show that the method is fast, accurate, and memory efficient. Finally, we show that the widely used DMFT is not valid for transverse variant ground compositions.

1 Introduction

Long-range propagation of the electromagnetic waves over the ground is a major topic for applications in communication, surveillance, or navigation. Models based on the parabolic wave equation (PWE) [1] are very popular in this context. The split-step Fourier (SSF) [1] method is a convenient way to solve the PWE.

The method is based on computing iteratively the field at increasing distances. At each step, the propagation is split into two parts. First, the propagation is performed in free space in the spectral domain. Second, effects of the atmosphere are introduced with a phase screen [1]. With this method, an impedance ground condition can be taken into account with the discrete mixed Fourier transform (DMFT) [2].

Recently, in 3D cylindrical coordinates, a discrete counterpart of SSF (DSSF) has been introduced [3] to obtain a self-consistent method. This allows avoiding spurious solutions. Nevertheless, the computation time and memory occupation prevent the operational use of the method.

Therefore, a wavelet-based split-step method (SSW) has been introduced in 2D [4, 5]. The fast wavelet transform (FWT) and the sparse representation with wavelets [6] yield a fast and memory-efficient method [5].

In this paper, an extension to 3D of SSW is proposed for the long-range propagation over any transverse invariant ground condition. Also, the ground wave propagation is considered. The relief is not considered here. Finally, we also show that the widely used DMFT does not work for transverse variant ground composition.

The article is organized as follows. In Section 2 the configuration and the discretization of the problem are described. In Section 3 a brief reminder on the discrete wavelet transform in 2D is introduced. In Section 4, we introduce the 3D split-step wavelet method. Besides numerical experiments are performed. In Section 5, we show that the DMFT does not work for transverse variant grounds. Section 6 concludes the paper.

2 Configuration and discretization

In this article, an $\exp(j\omega t)$ time dependence is assumed for the field. The problem is studied in Cartesian coordinates (x,y,z). Therefore, the scalar wave equation for the reduced field u [1] is defined as follows

$$\frac{\partial^2 u}{\partial x^2} - 2jk_0\frac{\partial u}{\partial x} + \frac{\partial^2 u}{\partial y^2} + \frac{\partial^2 u}{\partial z^2} + k_0^2 n^2 u = 0, \qquad (1)$$

with k_0 the free-space wave number and n the slowly varying refractive index. The main propagation axis is x. The z-axis corresponds to the altitude. We compute the forward propagation, $x \geq 0$, over the ground, $z > 0$, for the reduced field u. This latter is known at $x = 0$, the source is placed at $x_s \leq 0$.

For numerical reasons, the domain is of finite size $(x,y,z) \in [0,x_{\max}[\times[0,y_{\max}[\times[0,z_{\max}[$. In addition, the domain is first discretized along y and z with $y_{p_y} = p_y\Delta y \ \forall p_y \in [0,N_y - 1[$, and $z_{p_z} = p_z\Delta z \ \forall p_z \in [0,N_z - 1[$, where Δy and Δz are the steps. In this domain the reduced field u at position x is denoted by $u_x[p_y,p_z]$. A discretization along x is also applied with a step Δx.

3 The 2D discrete wavelet transform

Here, the 2D discrete wavelet transform on a separable wavelet basis [6] used to decompose the reduced field u_x is introduced. In image theory the wavelet transform and its associated fast transform are widely used, *e.g.* image compression.

The separable wavelet basis is composed of $3L+1$ functions, with L the maximum level of the decomposition. In 2D, three different wavelets, of zero mean, for the horizontal, vertical, and diagonal variations of the signal are used. All of them are dilated and translated to obtain a wavelet family. The dilations allow covering the spectrum, while the translations allow covering the spatial domain. These functions are denoted by $\psi_l^o[p_y,p_z]$, with $l \in [1,L]$ the level and $o \in \{h,v,d\}$ the orientation. The scaling function, denoted by ϕ_L, of non-zero mean is added to cover the lowest part of the spectrum. This latter is also translated to cover the spatial domain. An orthonormal basis is obtained.

The decomposition on this basis is then performed with the FWT [6]. The complexity of this algorithm, $O(N_yN_z)$, is lower than the fast Fourier transform (FFT). This allows a speed-up for the split-step method. A second advantage of the wavelet transform is that for a smooth signal, such as the one we deal with, the coefficients are fastly decreasing to 0 allowing a good sparse representation which is suitable for compression [6].

4 SSW over a transverse-invariant ground

In this section, we assume that the parameters of the ground are invariant along the transverse axis y.

4.1 Overview of the method

In this part, we introduce the SSW method in 3D. This latter iteratively computes the field by going back and forth in the spatial and wavelet domains.

One step of propagation from x to $x+\Delta x$ for u_x is performed as follows. Firstly, the wavelet coefficients are obtained from the field with a FWT (denoted by operator $\mathbf{W}$). Compression (operator $\mathbf{C}$) is applied to obtain a sparse set of coefficients. These coefficients are propagated in the wavelet domain with a propagator P. This step consists of propagating each non-zero coefficient by applying to each one a pre-computed local propagator.

To compute the set of propagators the method is a generalization of the 2D strategy [5]. This strategy is composed of three steps. First, for each level l and orientation o, a centered wavelet $\psi_{l,0}^o[p_y,p_z]$ is propagated on Δx with DSSF. To reduce the computation time this propagation is performed on the wavelet support [5]. The propagated wavelet $\psi_{l,\Delta x}^o[p_y,p_z]$ is obtained. Therefore, to compute all propagations, $3L+1$ DSSFs are needed. If $\Delta y = \Delta z$, then a rotation invariance property between the horizontal and vertical wavelet can be used to reduce this number to $2L+1$.

Second, the translation property described in 1D in [4] is used in both directions to efficiently obtain all the needed propagators. We denote by $p_{t_y}^l$ and $p_{t_z}^l$ the respective translations along y and z. Both depend on the level, since the space grid of the wavelet is dilated by two for each level. Thus, for $(p_{t_y}^l, p_{t_z}^l) \in [0,2^{L-l}[\times[0,2^{L-l}[$, the set of wavelets $\psi_{l,\Delta x}^o[p_y+p_{t_y}^l, p_z+p_{t_z}^l]$ is obtained. Third, FWT and compressions (with hard threshold V_p) are applied on each translated wavelet to obtain $P_{l,o,p_{t_y}^l,p_{t_z}^l}$, the elements of the set of local propagators.

The propagation is then performed with this set P as a sum of local operators translated and weighted by the nonzero coefficients $\alpha_l^0[p_y,p_z]$, such that

$$U_{x+\Delta x} = \sum_{l,o,p_y,p_z} \left(\alpha_l^o[p_y,p_z] P_{l,o,p_{t_y}^l,p_{t_z}^l}\right)[\cdot+p_y,\cdot+p_z], \quad (2)$$

with

$$p_{t_y}^l = p_y \pmod{2}^{L-l} \text{ and } p_{t_z}^l = p_z \pmod{2}^{L-l}, \quad (3)$$

where p_y,p_z,l and o are respectively the position along y and z, the level and the orientation of α.

The free-space propagated field is computed with an inverse FWT (denoted by $\mathbf{W}^{-1}$). Effects of the atmosphere are taken into account through a phase screen [1] (operator $\mathbf{D}$). This yields

$$u_{x+\Delta x} = \mathbf{D}\mathbf{W}^{-1}P\mathbf{C}\mathbf{W}u_x. \quad (4)$$

For more informations about the SSW algorithm and to the local strategy, we refer to [4, 5], respectively.

For a PEC ground condition, the local image method [4] is applied. This method consists of computing a local replica of the field in a thin image layer that simulates a reflection coefficient of value -1. The field and its image are then propagated. Finally, the local replica is cleared, thus avoiding spurious errors entering the computation domain. For an impedance condition, the DMFT [2] change of variable from u to w is computed beforehand. The local image method is then applied to w. The ground wave propagation is treated separately as for DSSF-DMFT [2].

Finally, an apodization layer is added at the top and at each side of the domain to avoid any reflection due to the finite size of the domain. Numerical experiments are now performed to test the method.

4.2 Canonical test

Here, we aim at comparing SSW to DSSF in terms of accuracy, computation time, and memory efficiency. The propagation over a planar dielectric ground in a vertical polarization is computed.

The configuration is as follows: the frequency is 300 MHz. The propagation is computed over 5 km with $\Delta x = 200$ m. The domain is of size 2048×2048 m in y and z directions, with $\Delta y = \Delta z = 1$ m. The source is a complex source point [7] placed at $x_s = -50$ m, with a waist size of $W_0 = 7$ m, $y_s = 1024$ m and $z_s = 50$ m. We assume an

impedance ground condition with parameters: $\varepsilon_r = 20$ and $\sigma = 0.02$ S/m. For the wavelet parameters, the symlet with $n_v = 6$ and a maximum level of decomposition $L = 3$ are used. The thresholds are $V_s = V_p = 0.002$.

In Figure 1 (a), we display the normalized fields (by its maximum) obtained with SSW. In (b), vertical cuts at $N_y/2$ of the final fields obtained with SSW and DSSF are plotted.

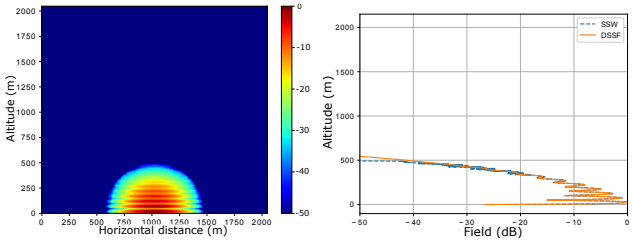

(a) Final normalized field (dB) obtained with lSSW in yOz-plane. **(b)** Vertical cuts at $N_y/2$ of the normalized final fields (dB).

Figure 1. Propagation of the field radiated by a CSP over a planar dielectric ground.

The final normalized error is of -31 dB. Also, the interference pattern is simulated with good accuracy, see Figure 1 (b). SSW is thus accurate with an impedance ground condition.

In terms of computation time and memory occupation, the results are summed up in Table 1. The propagator corresponds to the set of local propagators for SSW and to the diagonal operator for DSSF. The propagation memory occupation corresponds to storing the wavelet coefficients for SSW and to storing the field for DSSF.

method	DSSF	lSSW
propagator time (s)	138	6.4
propagation time (min)	32	32
propagator memory (MB)	604	5.6
propagation memory (MB)	604	0.05 to 2

Table 1. Computational cost of DSSF and lSSW in terms of time and memory occupation.

The first conclusion is that in terms of memory occupation, SSW is much more efficient. For the computation time, both SSW and DSSF take 32 min. If not faster, SSW allows computing the propagation with a drastically reduced memory occupation. This allows studying configurations with larger distances.

4.3 Millington effect

In this section, we study the configuration of Millington [8]. The configuration is y-invariant to show that the ground wave propagation can be accurately described with SSW in this case.

The configuration is as follows. The frequency is $f =$ 75 MHz, sufficiently low to have ground wave propagation effects. The domain is of size 5 km along x and 1024×1024 m in y and z directions. The steps are $\Delta x =$ 100 m and $\Delta y = \Delta z = 4$ m. We study a y-invariant source composed of CSP placed at $x_s = -50$ m and $z_s =$ with a waist of size $W_0 =$. The ground composition is described in Figure 2 and is the same as in [8]. The parameters are $\varepsilon_r = 20$ and $\sigma = 0.02$ S/m for the ground and $\varepsilon_r = 80$ and $\sigma = 5$ S/m for the sea. We expect to see the Millington recovery effect when reaching the sea. The wavelet parameters remain the same, with $V_s = V_p = 3.2 \times 10^{-4}$.

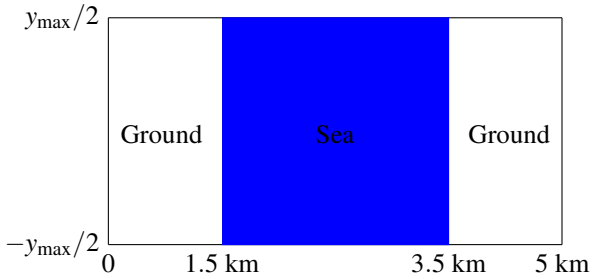

Figure 2. Scenario of propagation over the sea.

The results displayed in Figure 3. The normalized field (by its maximum) obtained with SSW is plotted in (a). In (b) the surface waves associated with the fields computed with 3D SSW and 3D DSSF are displayed.

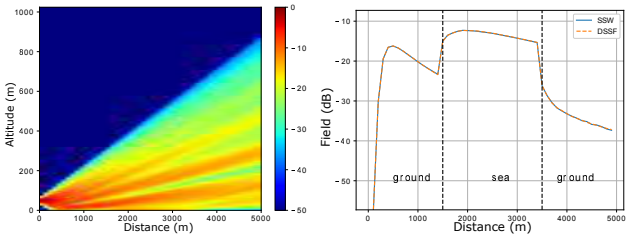

(a) Normalised field (dB) in $x0z$-plane obtained with 3D SSW. **(b)** Propagation of the field at $z = 0$ obtained with 3D lSSW and DSSF.

Figure 3. Propagation over a ground-sea-ground configuration.

First, the behavior for the surface wave corresponds to the one obtained in [8]. When reaching the sea, the Millington recovery effect is modeled, *i.e.*, the ground wave is increasing since ε_r and σ are high. Also, the final normalized difference between 3D DSSF and 3D SSW is -32 dB. We can see that below this value the DSSF and SSW ground waves are slightly different, due to the compressions in SSW.

Hence, we extend the conclusion of [5] showing that the 3D SSW method allows to model ground propagation with a surface wave more efficiently than 3D DSSF. Thus, 3D SSW can be used in complex environments.

5 The problem with transverse-variant grounds

In this section, the case of the propagation over the sea with islands is studied. We show that the popular DMFT [2]

method used with the split-step method does not work in this case. For conciseness, the continuous formulation is used here.

The common solution to account for a dielectric ground is the mixed Fourier transform (MFT) [9]. The change of variable from u to w is performed as

$$w_x(y,z) = \frac{\partial u_x(y,z)}{\partial z} + \alpha_x(y) u_x(y,z), \tag{5}$$

with α_x depending on y in this case. Cross-terms with α_x appears in the derivative along y in equation (1). Thus, w is not solution of a simple wave equation.

We now investigate the resolution of the propagation equation (1) with the reduced field u. Since the boundary condition in $z = 0$ depends on y, through $\alpha_x(y)$, an independent diagonalization along y and z is not possible to obtain the spectral representation.

Firstly, since periodic boundary conditions along y are assumed, we consider a diagonalization along y with a Fourier representation. In this case, the boundary condition at $z = 0$ becomes

$$\frac{\partial \tilde{u}_x(k_y,0)}{\partial z} + \left(\tilde{\alpha_x} \otimes \tilde{u_x}\right)(k_y,0), \tag{6}$$

with $\tilde{u}_x$ and $\tilde{\alpha}_x$ corresponding to the Fourier transforms of u_x and α_x along y and $\otimes$ to a convolution. This condition is not local, preventing an efficient resolution. Secondly, a diagonalization along z could be considered. The transform would correspond to the one used in the MFT [9], but the term α_x depends on y, also leading to convolutions.

Therefore, for a transverse variant ground composition, the split-step resolution is not accurate as is, and a new theory must be derived.

6 Conclusion

In this article, the SSW method has been extended to 3D for the long-range propagation over a transverse invariant impedance ground condition.

With this method, the propagation is computed iteratively by going back and forth in the wavelet and spatial domains. The ground is taken into account with the local image method for a PEC. For an impedance condition, the local image method is associated with the DMFT to take into account the ground and the surface waves accurately. With the FWT and the sparse representation allowed by wavelets, the method is memory- and time-efficient. Numerical tests have shown the method has a drastically lower memory occupation than DSSF while the computation time is of the same order. Also, the study of the Millington scenario has shown that the ground wave is accurately described for an infinite island along the transverse direction. Finally, we have shown that for finite islands the propagation can not be considered with the DMFT.

For future works, relief should be considered. Also, a new theory must be derived for transverse variant ground composition.

7 Acknowledgements

The authors would like to thank the French Defense Agency (Direction Général de l'Armement, DGA) and the French Civil Aviation University (Ecole Nationale de l'Avitation Civile, ENAC) for the funding.

References

[1] M. Levy, *Parabolic Equation Methods for Electromagnetic Wave Propagation*, IET, 2000.

[2] D. Dockery and J. R. Kuttler, " An improved impedance-boundary algorithm for Fourier split-step solutions of the parabolic wave equation," *IEEE Transactions on Antennas and Propagation*, **44**, pp. 1592–1599, 1996.

[3] H. Zhou, A. Chabory, and R. Douvenot. "A 3-D split-step Fourier algorithm based on a discrete spectral representation of the propagation equation," *IEEE Transactions on Antennas and Propagation,* **65(4)**, pp 1988–1995, 2017.

[4] H. Zhou, R. Douvenot, and A. Chabory. "Modeling the long-range wave propagation by a split-step wavelet method," *Journal of Computational Physics*, 402:109042, 2020.

[5] T. Bonnafont, R. Douvenot, and A. Chabory," A local split-step wavelet method for the long-range propagation simulation in 2D," *Radio Science,* 2021, in press.

[6] S. Mallat, *A Wavelet Tour of Signal Processing*, Academic press, 1999.

[7] G.A. Deschamps, "Gaussian beam as a bundle of complex rays," *Electronics Letters,* **23(7)**, pp 684–685, 1971.

[8] G. Millington, "Ground-wave propagation across a land/sea boundary," *Nature*, **163 (4134)**, pp 128–128, 1949.

[9] J.R. Kuttler, and G.D. Dockery, "Theoretical description of the parabolic approximation/Fourier split-step method of representing electromagnetic propagation in the troposphere," *Radio Science*, **26 (2)**, pp 381–393, 1991.